



# A Schwarz iterative method to evaluate ocean- atmosphere coupling schemes. Implementation and diagnostics in IPSL-CM6-SW-VLR

Olivier Marti<sup>1</sup>, Sébastien Nguyen<sup>1,2</sup>, Pascale Braconnot<sup>1</sup>, Sophie Valcke<sup>3</sup>, Florian Lemarié<sup>4</sup>, and Eric Blayo<sup>4</sup>

<sup>1</sup>Laboratoire des Sciences du Climat et de l'Environnement, LSCE/IPSL, CEA-CNRS-UVSQ, Université Paris-Saclay, Gif-sur-Yvette, France

<sup>2</sup>Now at Laboratoire d'Océanographie et du Climat : Expérimentations et Approches Numériques, Sorbonne Université / CNRS, France

<sup>3</sup>CECI, Université de Toulouse, CNRS, CERFACS, Toulouse, France

<sup>4</sup>Univ. Grenoble Alpes, Inria, CNRS, Grenoble INP, LJK, 38000, Grenoble, France

**Correspondence:** Olivier Marti (olivier.marti@lsce.ipsl.fr)

**Abstract.** State-of-the-art Earth System models, like the ones used in the CMIP6 intercomparison project, suffer from temporal inconsistencies at the ocean-atmosphere interface. Indeed, the coupling algorithms generally implemented in those models do not allow for a correct phasing between the ocean and the atmosphere, and hence between their diurnal cycles. A possibility to remove these temporal inconsistencies is to use an iterative coupling algorithm based on Schwarz methods. Despite the fact that the computational cost is large compared to standard coupling methods, which makes the method impractical as is for production runs, Schwarz algorithms are useful to evaluate some of the errors made in state-of-the-art ocean-atmosphere coupled models (e.g. in the representation of the processes related to diurnal cycle), as illustrated by the present study. A new coupling scheme based on such iterative method has been implemented in the IPSL coupled model. Comparisons between coupled solutions obtained with this new scheme and the standard IPSL coupling scheme show large differences at sunrise and sunset, when the external forcing (insolation at top of atmosphere) has the fastest pace of change. At these times of the day, the difference between the two numerical solutions is often larger than 100% of the solution, even with a small coupling time step, thus suggesting that significant errors are potentially made with current coupling methods. Most of those differences can be strongly reduced by making only two iterations of the Schwarz method which leads to a doubling of the computing cost. A thorough design of the first guess to initialize the iterative process may yield a solution that reduces the error with only one iteration. The present study focuses on the ocean-atmosphere interface, with no sea-ice. The problem with three components (ocean / sea-ice / atmosphere) remains to be investigated.

## 1 Introduction

For historical and physical reasons, present-day coupling algorithms implemented in ocean-atmosphere coupled models (CMs) are primarily driven by the necessity to conserve energy and mass at the air-sea interface. However the discretization of the coupling problem often leads to inconsistencies in time and space associated to the coupling algorithm and to the grid-to-grid interpolation of air-sea fluxes and temperatures. In time, the coupling algorithms currently used in state of the art CMs do



not provide the exact solution to the ocean-atmosphere problem, but an approximation of one. Indeed, these approaches are mathematically inconsistent in the sense that they do not allow for a correct phasing between the ocean and the atmosphere. Roughly speaking, the existing coupling algorithms used in CMs split the total simulation time into smaller time intervals (called coupling periods) over which averaged-in-time boundary data are exchanged. Over a particular coupling period, the average atmospheric fluxes are computed in the atmospheric model using the oceanic surface properties computed and averaged by the oceanic model over the previous coupling period. Therefore, for a given coupling period, the fluxes used by the oceanic model are not coherent with the oceanic surface properties considered by the atmospheric model. We will designate this method as 'lagged' in the rest of the paper, as the boundary conditions always lag the models.

Due to the overwhelming complexity of CMs, the consequences of inaccuracies in coupling algorithms on numerical solutions are hard to untangle, unless a properly (tightly) coupled solution can be used as a reference. Schwarz algorithms are attractive iterative coupling methods to cure the aforementioned temporal inconsistencies and provide tightly coupled solutions. As discussed in Lemarié (2008), the standard lagged coupling methods correspond to one single iteration of a global-in-time Schwarz Method (i.e. of what should be an iterative process). However, the theoretical analysis of the convergence properties of the Schwarz methods is restricted to relatively simple linear model problems (e.g. Gander et al., 1999; Gander and Halpern, 2007; Lemarié et al., 2013). More recently, Théry et al. (2020) analyzed the convergence for coupled one-dimensional Ekman layer problem, with vertical profiles of viscosities in both fluids. But there is no a priori guarantee that the iterative process converges in practice when implemented in tri-dimensional ocean-atmosphere coupled models.

Preliminary numerical experiments using the Schwarz coupling method for the simulation of a tropical cyclone with a realistic regional coupled model have already been carried out (Lemarié et al., 2014). Ensemble simulations were designed by perturbations of the initial conditions and of the length of the coupling period. One ensemble was integrated using the Schwarz method and another using a lagged method, as described previously. The Schwarz iterative coupling method led to a significantly reduced spread in the ensemble results (in terms of cyclone trajectory and intensity), thus suggesting that a source of error is removed with respect to the lagged coupling case. For these experiments the iterative process converges when coupling fully realistic numerical codes (Lemarié et al., 2014), which strengthens our belief that Schwarz methods can be a useful tool in the geophysical applications. Interestingly enough, a similar link between model uncertainties and consistency of the coupling method has been observed by Connors and Ganis (2011) on a coupled problem between two Navier-Stokes equations with interface conditions given by a bulk formulation.

The present study aims to assess the error made when using lagged coupling algorithms in state-of-the art CMs. To do so, a mathematically consistent Schwarz iterative method is implemented in the IPSL Earth system model. It is used as a reference to evaluate the error due to the lagged method. We study the convergence speed, and propose further developments in order to improve future ocean-atmosphere coupled models.

The paper is organized as follows. In section 2, we explain the lagged coupling, taking as an example the IPSL model, and the Schwarz iterative method. Section 3 describes the model and the experimental set-up. Section 4 analyses the results, in term of convergence speed and error assessment. Conclusion and future approaches are given in section 5.



## 2 State of the art of ocean-atmosphere coupling methods and Schwarz algorithms

Multiphysics coupling methods used in the context of Earth System models can be classified into two general categories (e.g. Lemarié et al., 2015; Gross et al., 2018). The first one (usually referred to as asynchronous coupling, and called 'lagged' in the present paper<sup>1</sup>) is based on an exchange of average fluxes between the models. The second one (referred to as synchronous coupling in Lemarié et al. (2015)) uses instantaneous fluxes. Climate modelling focuses primarily on how energy is exchanged between the Earth and the outer space, and is transported by the ocean and the atmosphere. When designing a coupling method in the context of CMs, water and energy conservation at the machine precision are the key features. Those conservation principles are tedious to satisfy when exchanging instantaneous fluxes. Coupled ocean-atmosphere models used for long-term integration (decades to millennia) all use a coupling methodology based on the exchange of time averaged or time integrated fluxes.

### 2.1 Current ocean-atmosphere coupling method in IPSL-CM6

Figure 1 describes how quantities are exchanged between the ocean and the atmosphere in the IPSL climate model from 1997 to now (Braconnot et al., 1997; Marti et al., 2010; Dufresne et al., 2013; Sepulchre et al., 2020; Boucher et al., 2020) knowing that both models are run in a concurrent way. The coupling time step  $\Delta t$  (which should not be confused with the dynamical time-step in the individual models) typically varies between 1 hour to 1 day, depending on the configuration and the model generation. Ocean and atmosphere dynamical time steps are always smaller, but commensurable with the coupling one. To describe this coupling strategy, we introduce the atmospheric state vector  $\mathcal{A}$  (encompassing temperature, humidity, pressure, velocity, ...) and the oceanic state vector  $\mathcal{O}$  (encompassing temperature, salinity, velocity, ...). The time evolution of the atmosphere and the ocean is symbolically described by

$$\frac{d\mathcal{A}}{dt} = \mathbf{F}_{\mathcal{A}}(\mathcal{A}, \mathbf{f}_{\Omega}), \quad \frac{d\mathcal{O}}{dt} = \mathbf{F}_{\mathcal{O}}(\mathcal{O}, \mathbf{f}_{\Omega}) \quad (1)$$

where  $\mathbf{F}_{\mathcal{A}}$  and  $\mathbf{F}_{\mathcal{O}}$  are partial differential operators including parameterizations, and  $\mathbf{f}_{\Omega}$  represents the fluxes at the ocean-atmosphere interface  $\Omega$ . This formulation is symmetric between the ocean and the atmosphere. But, in practice, in CMs the symmetry is broken between the fast atmospheric component and the slower oceanic component. The fluxes are generally computed by the atmospheric component or by an interface model, using oceanic surface quantities and atmospheric quantities taken in the vicinity of the air-sea interface (sea-surface properties are noted  $\mathcal{O}_{\Omega}$  in the following), meaning that (1) can be reformulated as

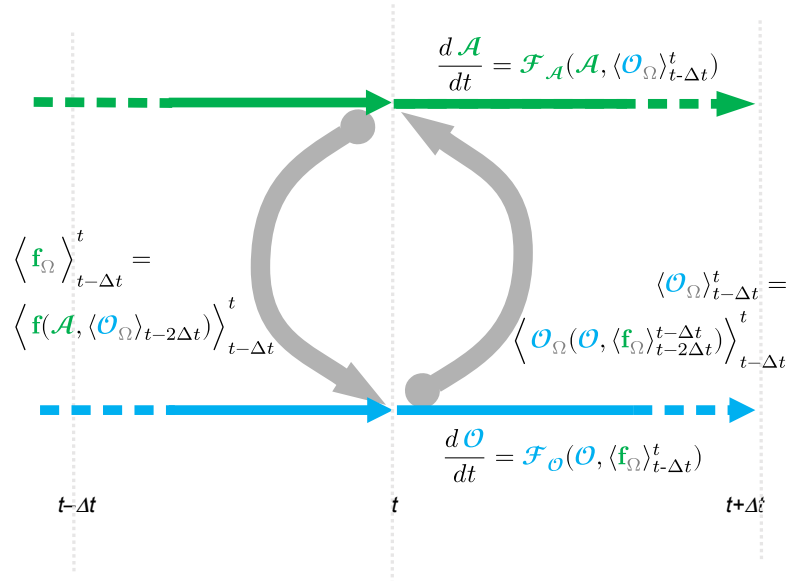
$$\frac{d\mathcal{A}}{dt} = \mathbf{F}_{\mathcal{A}}(\mathcal{A}, \mathcal{O}_{\Omega}), \quad \frac{d\mathcal{O}}{dt} = \mathbf{F}_{\mathcal{O}}(\mathcal{O}, \mathbf{f}_{\Omega}), \quad \mathbf{f}_{\Omega} = \mathbf{f}_{\Omega}(\mathcal{A}, \mathcal{O}_{\Omega}) \quad (2)$$

With such an approach, the atmospheric model receives surface properties like sea surface and sea-ice surface temperature, fraction of sea-ice, albedo and velocities of the surfaces (sea water and sea ice) and computes its own interfacial fluxes which

<sup>1</sup>The terms "synchronous" and "asynchronous" may have a total different signification for climate modellers, and we prefer to avoid them.



**Figure 1.** Time stencil of the exchanges between the ocean and the atmosphere in IPSL models, when the legacy lagged method is used. Redrawn from Fig. 5.4 of Lemarié (2008).



85 are then sent to the oceanic component. Interfacial fluxes sent by the atmosphere include heat fluxes (radiative and turbulent), water fluxes (solid and liquid precipitation, evaporation, sublimation) and momentum fluxes (wind stress).

As mentioned earlier, the coupling algorithm in the IPSL climate model is based on an exchange of averaged-in-time fluxes. We define  $\langle \dots \rangle_{t_1}^{t_2}$  as the time average in the interval  $[t_1, t_2]$ , and  $\Delta t$  the coupling time step (*i.e.* the duration of a coupling period). A schematic view of the exchanges between the ocean and the atmosphere is given in Fig. 1. To run over a coupling  
 90 period  $\Delta t$ , each component uses the available boundary conditions which are time averaged from the previous coupling period; over the interval  $[t, t + \Delta t]$ , we thus have:

$$\frac{d\mathcal{A}}{dt} \Big|_t^{t+\Delta t} = \mathbf{F}_{\mathcal{A}}(\mathcal{A}, \langle \mathcal{O}_{\Omega} \rangle_{t-\Delta t}^t), \quad \frac{d\mathcal{O}}{dt} \Big|_t^{t+\Delta t} = \mathbf{F}_{\mathcal{O}}(\mathcal{O}, \langle \mathbf{f}_{\Omega} \rangle_{t-\Delta t}^t) \quad (3)$$

To be more precise, the fluxes sent from the atmosphere to the ocean and the surface properties sent from ocean to atmosphere at time  $t$  are :

$$95 \quad \langle \mathbf{f}_{\Omega} \rangle_{t-\Delta t}^t = \left\langle \mathbf{f}_{\Omega}(\mathcal{A}, \langle \mathcal{O}_{\Omega} \rangle_{t-2\Delta t}^{t-\Delta t}) \right\rangle_{t-\Delta t}^t, \quad \langle \mathcal{O}_{\Omega} \rangle_{t-\Delta t}^t = \left\langle \mathcal{O}_{\Omega}(\mathcal{O}, \langle \mathbf{f}_{\Omega} \rangle_{t-2\Delta t}^{t-\Delta t}) \right\rangle_{t-\Delta t}^t \quad (4)$$

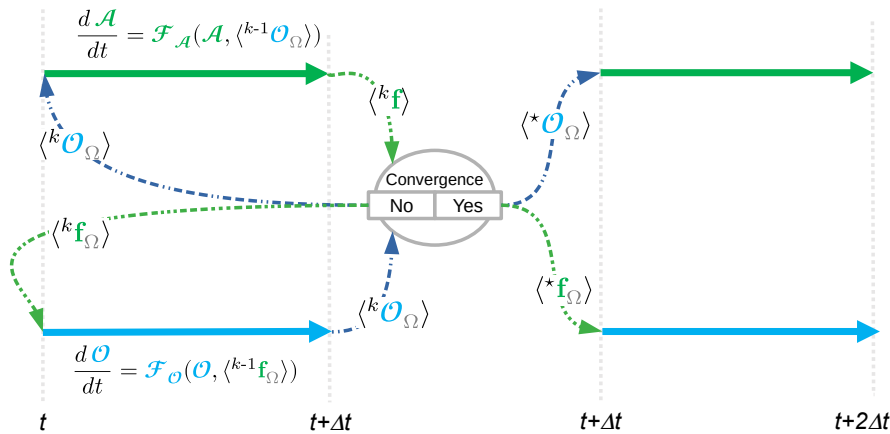
Substituting (4) in (3), we thus can write the evolution of the ocean  $\mathcal{O}$  and the atmosphere  $\mathcal{A}$  from  $t$  to  $t + \Delta t$  as :

$$\frac{d\mathcal{O}}{dt} \Big|_t^{t+\Delta t} = \mathbf{F}_{\mathcal{O}} \left( \mathcal{O}, \left\langle \mathbf{f}(\mathcal{A}, \langle \mathcal{O}_{\Omega} \rangle_{t-2\Delta t}^{t-\Delta t}) \right\rangle_{t-\Delta t}^t \right), \quad \frac{d\mathcal{A}}{dt} \Big|_t^{t+\Delta t} = \mathbf{F}_{\mathcal{A}} \left( \mathcal{A}, \left\langle \mathcal{O}_{\Omega}(\mathcal{O}, \langle \mathbf{f}_{\Omega} \rangle_{t-2\Delta t}^{t-\Delta t}) \right\rangle_{t-\Delta t}^t \right) \quad (5)$$

The interfacial flux used as a boundary condition for the ocean between  $t$  and  $t + \Delta t$  is computed using surface values of the ocean from the time range  $[t - 2\Delta t, t - \Delta t]$ . Symmetrically, the sea-surface properties used to run the atmosphere between  $t$  and



**Figure 2.** Stencil of the Schwarz iterative method.  $k$  is the iteration number. The  $*$  superscript denotes the converged solution. At each iteration  $k$ , the initial states of  $\mathcal{O}$  and  $\mathcal{A}$  are reset to the same initial value, which is the converged solution of the previous coupling time step  $[t - \Delta t, t]$ . Only the boundary conditions are updated at each iteration.



100  $t + \Delta t$  are computed using surface values of the ocean from the time range  $[t - 2\Delta t, t - \Delta t]$ . Eq. (4) and Eq. (5) demonstrate the time shift between the two models, and how the boundary conditions lag the models. The numerical solution thus obtained is not mathematically consistent and suffers from synchronicity issues which ultimately may yield the numerical implementation to be unstable in the sense that the error compared to the exact solution keeps increasing with time.

To our knowledge, no coupled ocean-atmosphere model uses a coupling algorithm that is mathematically consistent. The  
 105 survey of actual use cases (Valcke, personal communication) shows that they all induce a time lag between the models and the boundary conditions, at least in one direction. In the GFDL Earth system model, the FMS coupler offers the possibility to use an implicit scheme to compute the interface quantities. But only the vertical turbulent diffusion part of the ocean and atmosphere models are considered (Balaji et al., 2006), and the full model equations are not synchronised.

## 2.2 The Schwarz iterative method

110 The Schwarz iterative method is described and analyzed in Lemarié et al. (2015) in the context of ocean-atmosphere coupling. The basic idea is to separate the global coupled problem on  $\mathcal{A} \cup \mathcal{O}$  into separated sub-problems on  $\mathcal{A}$  and  $\mathcal{O}$ , which can be solved separately with an appropriate exchange of boundary conditions at the common interface  $\Omega$ . An iterative process is applied to achieve the convergence to the solution of the global problem. The main concern about this approach is the computational cost which directly depends on the convergence speed. As illustrated in Fig. 2, we iterate the system until  
 115 convergence over the time interval  $[t, t + \Delta t]$ . The first guesses of  $\mathcal{A}$  and  $\mathcal{O}$  at time  $t$  are taken from the coupling time step



$[t - \Delta t, t]$ . The iterative process from iteration  $k - 1$  to iteration  $k$  is described by:

$$\begin{cases} \frac{d^k \mathcal{A}}{dt} = \mathbf{F}_{\mathcal{A}}({}^k \mathcal{A}, \langle {}^{k-1} \mathcal{O}_{\Omega} \rangle) \\ \frac{d^k \mathcal{O}}{dt} = \mathbf{F}_{\mathcal{O}}({}^k \mathcal{O}, \langle {}^{k-1} \mathbf{f}_{\Omega} \rangle) \\ {}^k \mathbf{f}_{\Omega} = \mathbf{f}_{\Omega}({}^{k-1} \mathcal{A}, \langle {}^{k-2} \mathcal{O}_{\Omega} \rangle) \\ {}^k \mathcal{O}_{\Omega} = \mathcal{O}_{\Omega}({}^{k-1} \mathcal{O}, \langle {}^{k-2} \mathbf{f}_{\Omega} \rangle) \end{cases} \quad (6)$$

For a state-of-the-art CM with complex parameterizations, we have no mathematical evidence that the algorithm converges. Indeed, as mentioned in Keyes et al. (2013), reaching a tight coupling between the components to be coupled requires smoothness. However, both ocean and atmosphere models include parameterizations that are potentially not differentiable. This is for instance the case of the bulk formulas used to compute the turbulent fluxes at the air-sea interface (e.g. Pelletier et al., 2018). A first step is thus to test the convergence when coupling realistic models. Assuming that the algorithm converges, for large values of  $k$  we would have  ${}^{k-1}(\mathcal{A} \cup \mathcal{O}) = {}^k(\mathcal{A} \cup \mathcal{O}) = {}^*(\mathcal{A} \cup \mathcal{O})$ , with the left superscript  $*$  denoting the converged solution. The evolution of  ${}^* \mathcal{O}$  and  ${}^* \mathcal{A}$  is given by:

$$\frac{d^* \mathcal{O}}{dt} \Big|_t^{t+\Delta t} = \mathbf{F}_{\mathcal{O}} \left( {}^* \mathcal{O}, \left\langle \mathbf{f}({}^* \mathcal{A}, \langle {}^* \mathcal{O}_{\Omega} \rangle_t^{t+\Delta t}) \right\rangle_t^{t+\Delta t} \right), \quad \frac{d^* \mathcal{A}}{dt} \Big|_t^{t+\Delta t} = \mathbf{F}_{\mathcal{A}} \left( {}^* \mathcal{A}, \left\langle {}^* \mathcal{O}_{\Omega}({}^* \mathcal{O}, \langle {}^* \mathbf{f}_{\Omega} \rangle_t^{t+\Delta t}) \right\rangle_t^{t+\Delta t} \right) \quad (7)$$

where it is clear that models and boundary conditions are now fully synchronized, meaning that the algorithm is mathematically consistent.

The Schwarz iterative procedure may span several coupling time steps. The time interval  $[t, t + \Delta t]$  is then called the 'Schwarz window'. It is divided in  $p$  coupling time steps. At the end of each Schwarz window, the models send the boundary conditions as a vector of values for the coupling intervals  $[t, t + \frac{1}{p} \Delta t]$ ,  $[t + \frac{1}{p} \Delta t, t + \frac{2}{p} \Delta t]$ , ...,  $[t + \frac{p-1}{p} \Delta t, t + \Delta t]$ . The boundaries conditions exchanged between the models are then vector of quantities :

$$\mathbf{f}_{\Omega} = \left\{ \langle \mathbf{f}_{\Omega} \rangle_t^{t+\frac{1}{p} \Delta t}, \langle \mathbf{f}_{\Omega} \rangle_{t+\frac{1}{p} \Delta t}^{t+\frac{2}{p} \Delta t}, \dots, \langle \mathbf{f}_{\Omega} \rangle_{t+\frac{p-1}{p} \Delta t}^{t+\Delta t} \right\}, \quad \mathcal{O}_{\Omega} = \left\{ \langle \mathcal{O}_{\Omega} \rangle_t^{t+\frac{1}{p} \Delta t}, \langle \mathcal{O}_{\Omega} \rangle_{t+\frac{1}{p} \Delta t}^{t+\frac{2}{p} \Delta t}, \dots, \langle \mathcal{O}_{\Omega} \rangle_{t+\frac{p-1}{p} \Delta t}^{t+\Delta t} \right\} \quad (8)$$

More details about the technical implementation in an Earth System Model are given in section 3.3. The following study handles only the case with the Schwarz window is equal to the coupling time step ( $p = 1$ ). The possibility to have a longer Schwarz window has not been coded for the sake of simplicity.

### 3 Model description

#### 3.1 The IPSL-CM6-SW-VLR version of the IPSL Earth system model

At the start of this study, IPSL had two operational Earth System Models available, IPSL-CM5A2-LR and IPSL-CM6-LR. IPSL-CM5A2-LR is an upgrade of IPSL-CM5A-LR (Marti et al., 2010; Dufresne et al., 2013) used by IPSL for the CMIP5



140 intercomparison exercise, made by Sepulchre et al. (2020). Compared to IPSL-CM5A-LR, the atmospheric model is tuned to reduce the surface cold bias and enhance the Atlantic meridional overturning circulation. The atmospheric code includes a supplemental level of shared memory parallelization that strongly improves the model scalability and speed. This model has an atmospheric resolution of  $3.75^\circ \times 1.875^\circ$  in longitude-latitude and 39 vertical levels. It has an oceanic resolution of 2 degrees and 31 vertical levels in the ocean. It runs at 70 simulated years per wall-clock day.

145 IPSL-CM6-LR (Boucher et al., 2020) is the model used by IPSL for the CMIP6 intercomparison exercise. It has a higher resolution in both ocean and atmosphere. All components (ocean, atmosphere, sea-ice and land surface) has been improved with better physics compared to IPSL-CM5A2-LR. It runs at 10 simulated years per wall-clock day. IPSL-CM6-LR computer code and running environment brings to the user a strong improve in term of performance, portability, readability, versatility and quality control. See Boucher et al. (2020) for details.

150 The present study uses the codes of IPSL-CM6, but runs at the resolution of IPSL-CM5A2-LR. As an iterative Schwarz method strongly increases the computing time, the choice of a low resolution allows to contain the computing cost. As we planned high difficulties to implement the Schwarz method in the old style coding of IPSL-CM5A2-LR, the choice of the newer code appeared obvious.

The parameters of the atmospheric model allow to reproduce exactly the atmosphere of IPSL-CM5A2-LR when atmosphere  
155 is run in standalone mode. In the ocean, the sea-ice model LIM3 is used with one category of ice (IPSL-CM6-LR uses 5 ice categories, based on ice thickness; see Rousset et al. (2015) for more details for LIM3 in mono category). The land surface model ORCHIDEE was removed to simplify and speed up the implementation of the Schwarz algorithm. As a soil model, we use the simple bucket model included in the atmosphere code.

This specific version of the model is called IPSL-CM6-SW-VLR for further reference, SW standing for Schwarz.

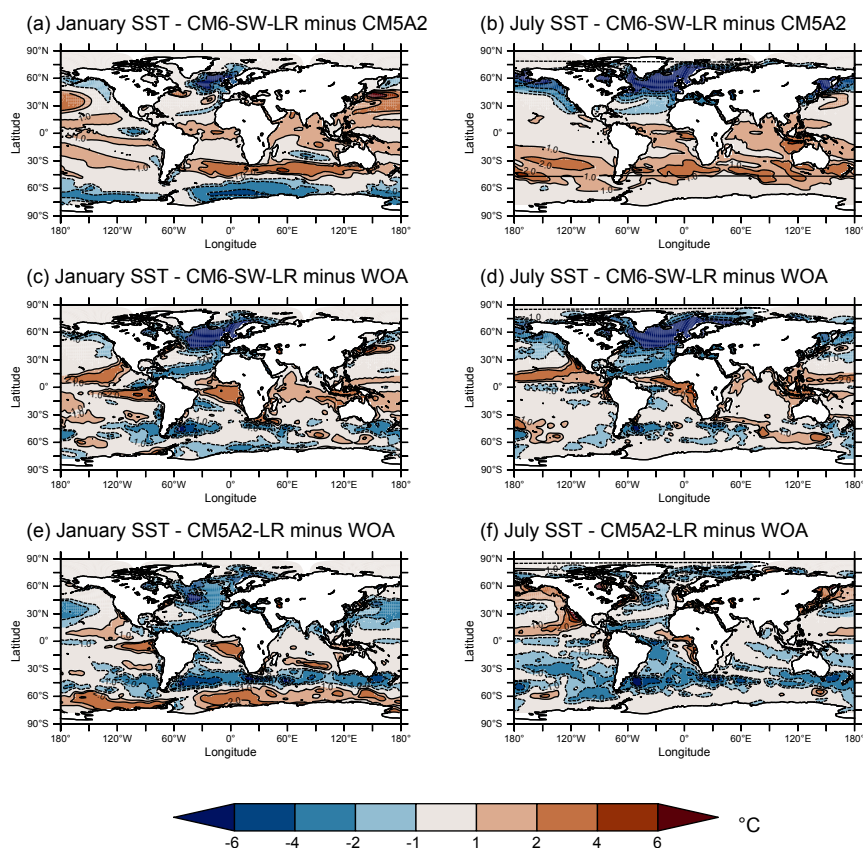
### 160 3.2 Evaluation of IPSL-CM6-SW-VLR

IPSL-CM6-SW-VLR simulated climate has substantial differences with IPSL-CM5A2-LR, due to the different soil and sea ice models. We present here a short evaluation of the simulated climate of a steady-state pre-industrial simulation. The initial state for the ocean of the atmosphere is taken from the reference IPSL-CM5A2-LR simulation of Sepulchre et al. (2020). For the ice model, LIM2 and LIM3 states are not compatible. In the present case, the sea-ice initial state is set to a fixed height of ice  
165 where the ocean temperature of the first level (at 5 m depth) is at the freezing point. The height of ice is 3 m in the northern hemisphere and 1 m in the south. On land the albedo parameters of the bucket model was taken from the albedo computed by ORCHIDEE in the reference PREIND simulation of Sepulchre et al. (2020), which follows the CMIP6 intercomparison project of the *piControl* experiment (Eyring et al., 2016). In a first attempt, the model evolves towards a cold state, due to an imbalance of about  $-2.8 \text{ Wm}^{-2}$  of the radiation budget at the top of the atmosphere (TOA).

170 The procedure described by Sepulchre et al. (2020) has been used to equilibrate the model. A parameter controlling the conversion of cloud water to rainfall is tuned to reach a near zero net flux at top of the atmosphere (TOA), with a target of  $13.5^\circ\text{C}$  for global mean near surface temperature (temperature at 2 m height). The final TOA heat budget is  $0.33 \text{ Wm}^{-2}$ , with



**Figure 3.** Sea surface temperature (SST) difference between the different versions of IPSLCM, and with the World Ocean Atlas. Left: January, right: July. Top : IPSLCM6-SW-LR minus IPSLCM5A2-LR, middle: IPSLCM6-SW-LR minus the World Ocean Atlas, bottom: IPSLCM5A2-LR minus the World Ocean Atlas (WOA, Locarnini et al., 2013).



a global mean near surface temperature of 13.3 °C. Figure 3 shows the simulated sea surface temperature (SST) compared to Sepulchre et al. (2020) and to the World Ocean Atlas (WOA, Locarnini et al., 2013).

175 As expected from the drastic simplification of the soil model, the performances, in term of simulated climate, of IPSLCM6-SW-VLR are poorer than those of the state-of-the models participating for example in the CMIP6 intercomparison exercise. But as the objective of this study focuses on the evaluation of the Schwarz method, a model with a perfect simulated climate is not necessary. We estimate that a good part of the degradation of this version compared to IPSL-CM5A2 is linked to the soil model.





**Table 1.** Main characteristics of experiments

Name	Coupling time step	Schwarz iterations
Sw1h1i	$\Delta t = 1$ h	1 (= No Schwarz)
Sw1h50i	$\Delta t = 1$ h	50
Sw4h1i	$\Delta t = 4$ h	1 (= No Schwarz)
Sw4h50i	$\Delta t = 4$ h	50

### 180 3.3 Implementation of the Schwarz algorithm in IPSL-CM6

The base of the Schwarz iterative algorithm is to repeat each coupling time step with the same initial condition for each iteration, but with changing boundary conditions at the ocean-atmosphere interface  $\Omega$  at each iteration, with the one produced by the previous iteration. IPSL-CM are restartable models: they produce the same result (bitwise) when run in one chunk, or when the run is splitted in small chunks, with the final state of each chunk written to disk and read by the following one. In the ocean and atmosphere codes, we implement the possibility to save/restore the fields needed for a restart to/from the computer memory.

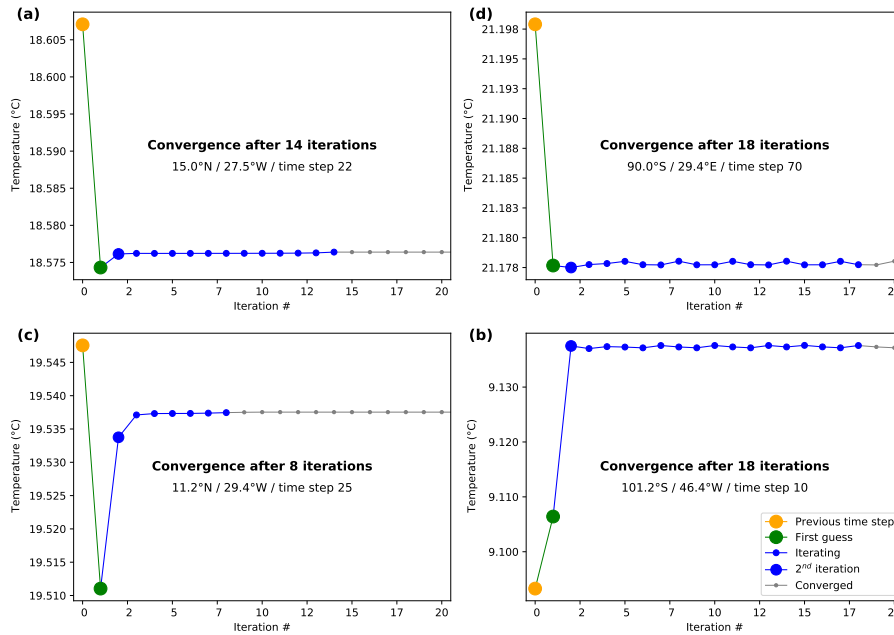
The time loop of the models are replaced by three intricated loops. The external one loops on coupling periods. The middle one loops over Schwarz iterations. The inside one loops over the model time steps inside a coupling period. (For a coupling time step of  $\Delta t = 1$  h, the ocean performs 2 time steps and the atmosphere 6 time steps for the vertical physics, 30 for the dynamics and 1 for the radiation scheme). An additional Schwarz loop is then added inside the time loop. At the first Schwarz iteration of a coupling time step, the initial states of the atmosphere  $\mathcal{A}$  and the ocean  $\mathcal{O}$  comes from the previous coupling time step. This state is saved in memory, and read at the beginning of each iteration to initialize  $\mathcal{A}$  and  $\mathcal{O}$  with the same state at each Schwarz iteration. At the end of each iteration, the boundary conditions are send to the companion model for use during the next iteration. The boundary conditions evolves during the iterative process. In this implementation, the length of the Schwarz window must equals the coupling period.

### 3.4 Experiments

We have run 4 experiments (see Table 1), with and without Schwarz iterations, and with coupling time steps of  $\Delta t = 1$  h and  $\Delta t = 4$  h. The number of iterations is fixed to 50. The experiments with Schwarz are run twice, one with outputs of model results at iteration 1, and the other one with outputs at iteration 50. The I/O system of the model is indeed not tailored to write a field several times at the same calendar time. The coupling fields exchanged between the models are written out at all iterations by the coupler OASIS, which allow us to study the convergence. Experiments are 5-day long (*i.e.* 120 and 30 Schwarz and coupling time steps). The initial state is the end of a fifty year control experiment with pre-industrial forcings, run with the legacy lagged method.



**Figure 4.** Behaviour of the sea surface temperature for four selected cases (i.e. instances of the Schwarz algorithm in space  $\times$  time). For each graph, the yellow dots show the values at the end of the previous coupling time step, which is the initial state of the present step. The green dots show the values after the first iteration. It is the value that the models use with the lagged method. The blue dots show the iterative process. Dots become grey when  $T_{\Omega}$  is considered to be converged. The two top cases (a) and (b) come from the  $\Delta t = 4$  h experiment. The bottom cases (c) and (d) come from the  $\Delta t = 1$  h experiment.



## 4 Results

### 205 4.1 Convergence

Figure 4 shows the behaviour of the sea surface temperature  $T_{\Omega}$  along the iterative process for four selected cases in time and space. These cases represent typical behaviours. The yellow dots show the values at the end of the previous time step. The green dots show the values after the first iteration. It is the values that the models would compute without Schwarz. The blue dots show the iterative process. Dots become grey when  $T_{\Omega}$  is considered to be converged.

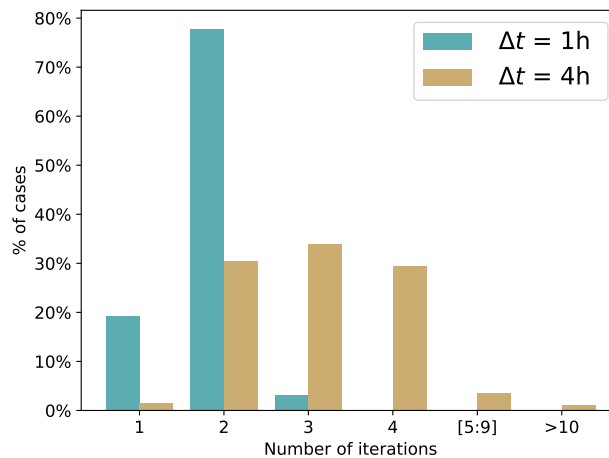
210 To decide if the convergence is reached at iteration  $k_{conv}$ , we consider  $A_{T_{\Omega}}(k)$ , the amplitude of the  $T_{\Omega}$  changes after the iteration  $k$ .  $A_{T_{\Omega}}(k) = \max_k^{k=50}(T_{\Omega}) - \min_k^{k=50}(T_{\Omega})$ . The convergence criterion is fulfilled if :

- Oscillation from iteration  $k_{conv}$  to 50 has an amplitude which is negligible in front of the total range of the signal, i.e. if  $A_{T_{\Omega}}(k_{conv}) \leq 10^{-3} A_{T_{\Omega}}(1)$

- Oscillation has an amplitude from iteration  $k_{conv}$  to 50 which is not bigger than the amplitude from iteration 41 to 50, i.e.  $A_{T_{\Omega}}(k_{conv}) \leq A_{T_{\Omega}}(40)$ . This last criterion supposes that convergence is always reached at iteration  $k = 40$ . For points 215 free of the sea-ice, this criterion is never necessary.



**Figure 5.** Number of iterations for convergence for the  $\Delta t = 1$  h and  $\Delta t = 4$  h simulations. The total number of cases is  $536,800 = 120$  time steps  $\times 4,553$  ice free grid points in the  $\Delta t = 1$  h simulation. And  $136,800 = 30$  time steps  $\times 4,560$  ice free grid points in the  $\Delta t = 4$  h simulation. The ordinates show the number of cases in percentage of the total number of cases in time  $\times$  space.



- Final oscillation from iteration  $k = k_{conv}$  to  $k = 50$  has an amplitude  $A_{\Omega}(k_{conv})$  always lower than  $10^{-4}$  °C for temperature,  $10^{-2}$   $Wm^{-2}$  for heat fluxes.

The speed of convergence is sensitive to the definition of these criteria, which mostly come from a 'rule of the thumb' rather than from a rigorous mathematical analysis. A small residual oscillation is observed at all cases. The mathematics of the Schwarz method for the ocean-atmosphere coupling has been developed in Lemarié (2008), Lemarié et al. (2014, 2015) or Théry et al. (2020). The theory is robust and well establish for two fluids with fixed turbulent viscosities. We have no theoretical frame when a third medium, sea-ice in our case, is present. In all of the following, we will not analyse the behaviour of the model when sea-ice is present, and study only ice-free points. Text and figures present the behaviour of the sea-surface temperature. We have checked that other interface variables (i.e. fluxes) converge at the same pace than the temperature.

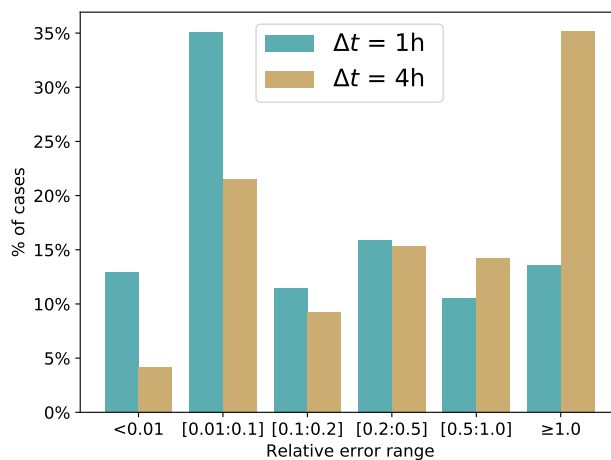
For case (a) of Fig. 4, the first iteration explains almost all the signal. The second iteration brings a small oscillation, then the solution starts to oscillate with a small amplitude. For case (b), the first iteration is even closer to the final solution. Cases (c) and (d) show that the Schwarz method can yield a solution that deviates substantially from the solution without Schwarz.

Figure 5 shows an histogram of the number of iterations. We consider all the instances of the iterative procedures, for each ocean point of the atmosphere grid, and for each coupling time step. As explain above, we consider only points with no sea ice.

In the  $\Delta t = 1$  h simulation, the Schwarz algorithm converges at the first iteration in almost 20% of the cases. Two iterations are enough in almost 80% of the cases. Only of few percents of cases require more iterations. For the  $\Delta t = 4$  h simulation, convergence is rarely reached in 1 iteration. In most of the cases 2 to 4 iterations are required. But the number of iterations might be sensitive to the choice of the convergence criterion. In the following, we diagnose the difference between the solutions with and without Schwarz, which does not depend on an arbitrary criterion.



**Figure 6.** Relative error of the change of sea surface temperature during a coupling time step. The error is computed as the ratio between i) the correction due to the iterative procedure (the jump from green dots to converged solution in grey in Fig. 4) and ii) the solution change between  $t$  to  $t + \Delta t$  with no Schwarz iteration (the jump from yellow to green dots in Fig. 4). See legend for Fig. 5 for the explanation of ordinate axis.



## 4.2 Diagnosing the error of lagged coupling

Figure 6 shows the relative error in the change of sea surface temperature during one coupling time step, made when the Schwarz method is not used. The error is computed as the ratio between i) the correction due to the iterative procedure (the jump from green dots to converged solution in grey in Fig. 4) and ii) the solution change between  $t$  to  $t + \Delta t$  with no Schwarz iteration (the jump from green to yellow dots in Fig. 4). In the  $\Delta t = 1\text{h}$  simulation, the relative error made in the lagged method is small (less than 0.1) in almost half of the cases. But it is larger than 0.1 for the other half. The relative error is even larger than 0.5 in 25 % of the cases. In the  $\Delta t = 4\text{h}$  simulation, small errors occurs in a minority of cases, and the error is larger than 0.5 in almost 50 % of the cases.

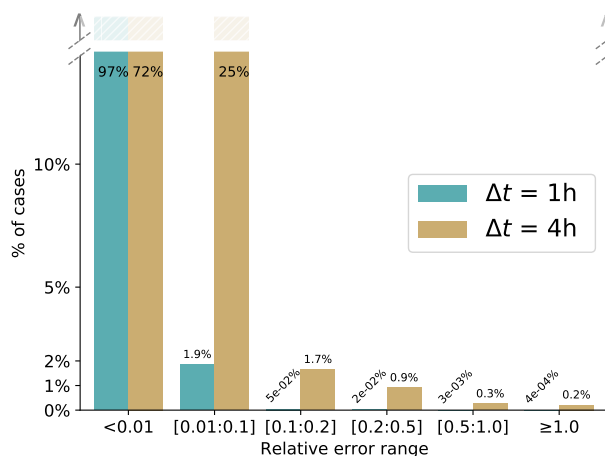
Figure 7 shows the relative error that would remain if we had stopped the Schwarz method at 2 iterations. The histogram shows that for the  $\Delta t = 1\text{h}$  simulation, non negligible errors ( $> 0.01$ ) account for about 2 % of the cases. For small coupling time steps, a two iterations Schwarz method strongly improves the solution compared to the lagged method, with only a handful of cases that need more than 5 iterations to reach a small error (less than 0.1, not shown). All these points are at the ice edge, where the convergence is slower. For  $\Delta t = 4\text{h}$ , 25 % of the cases have an error in the range  $[0.01, 0.1]$ . The number of cases with error larger than 0.1 after 2 iterations amounts to about 3.5 %. This is still a large improvement compared to the lagged method.

## 4.3 The diurnal cycle

Figure 8 plots the error in function of local time and error classes. The error histograms show a well-defined diurnal cycle with the lowest errors in the middle of the night. In both experiments, but mostly for  $\Delta t = 4\text{h}$ , errors are larger at noon than



**Figure 7.** Same as Fig. 6, but with the relative error computed between the final iterated solution and the solution obtained after 2 iterations. See legend for Fig. 5 for the explanation of ordinate axis. The ordinate axis is cut at 15 % to focus on non negligible errors.



at midnight. The error is maximum around sunset and sunrise, when the change of the insolation forcing evolves at the fastest  
 255 pace. This pattern is clear for  $\Delta t = 1\text{h}$ . With  $\Delta t = 4\text{h}$ , the diurnal cycle of insolation is badly resolved, but the diurnal cycle  
 of the error is still present. At sunrise and sunset, 45% of cases in time  $\times$  space show an error larger than 1 for the  $\Delta t = 1\text{h}$   
 case. At these times of the day more than 70% of the cases show error larger than 0.5, and almost all cases have non negligible  
 errors ( $\geq 0.01$ ). All figures are slightly bigger for the  $\Delta t = 4\text{h}$  case.

An error larger than 1.0 means that the correction due to the Schwarz method is larger than the solution jump due to the  
 260 lagged method. In both simulations the error of the lag method around sunrise and sunset can be the most important part of the  
 solution computed by an Earth System model.

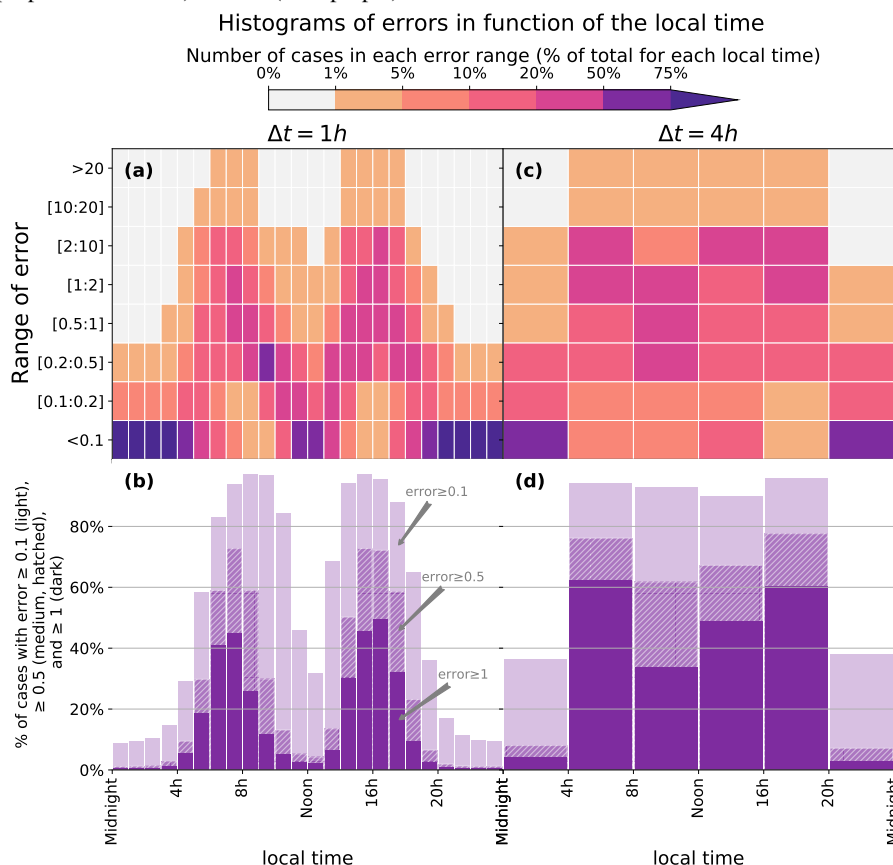
## 5 Conclusions and future approaches

Present time schemes used to couple ocean and atmosphere in state-of-the-art Earth System Model are mathematically in-  
 consistent, as the components are not correctly synchronized with their boundary conditions (Lemarié, 2008; Lemarié et al.,  
 265 2014). A mathematically consistent Schwarz iterative method has been implemented in the IPSL coupled model, to solve the  
 ocean-atmosphere interface. This implementation yields a multiplication of the computing cost by the number of iterations.  
 Although such a method is thus not affordable as is for climate studies, the Schwarz iterative method is used as a reference to  
 evaluate the error made with the legacy lagged method currently used by many ocean-atmosphere modelers.

We use the solution with the Schwarz iterative method as a reference to diagnose the error in two experiences where only  
 270 the coupling time step  $\Delta t$  differs. This error is quite large, with highest values around dawn and dusk, when the change of  
 insolation at the top of the atmosphere, the only external forcing, has the highest rate. With the shortest time step of  $\Delta t = 1\text{h}$ ,



**Figure 8.** Histograms of errors as a function of the local time and error classes. Left panels for  $\Delta t = 1$  h, right panels for  $\Delta t = 4$  h. Top panels shows the percentage of cases in space  $\times$  time in each range of error, as a function of the local time. The percentages are computed with respect to the total number of cases for each local time. Bottom panels show the number of cases with errors larger than 0.1 (light purple), 0.5 (medium purple with hatches) and 1.0 (dark purple).



45% of the cases in time  $\times$  space show an error larger than 100%. That means that for this time of the daily cycle, the solution without Schwarz suffers from a large error in most of the cases. With a larger coupling time step, the errors are even larger.

The error can be strongly reduced by performing only two iterations. This is still a huge increase of the computing cost, which is clearly unacceptable. A Schwarz method is affordable only if the number of iteration is kept to one. In the normal case, a one iteration Schwarz method is equivalent to the legacy lagged method. But we can improve it by using a better first guess than the solution of the previous time step. We could for instance perform Schwarz iterations on a sub part of the model, to get an improved first guess before running the full model once. It will be effective if we can identify parts of the models that represent only a small part of the calculation cost, but account for a large part of the total solution.

With two iterations, a conservation issue appears. The second, and last, iteration of the ocean model uses the fluxes computed by the atmosphere during the first iteration. The atmosphere will get its energy and water balance from the fluxes computed at



the second iteration. Both components do not use the same fluxes, which yield a conservation inconsistency at the interface. This happens when the iteration process is stopped before the full convergence. In this case, the ocean model would have to run one more iteration than the atmosphere, to close the energy and water cycle between the model components.

285 In the GFDL Earth system model, the FMS coupler allows to use an implicit scheme to compute the interface quantities, but only the vertical diffusivity is computed. We assume that this implicit scheme on a sub part of the model can reduce the total error. This method is not implementable in IPSL-CM6 in an easy way. In IPSL-CM6, it is possible to share the Schwarz iterations in two phases. In the first phase, only a sub part of the model is computed. This first phase, with a reduced computing cost, can provide an improved initial guess for the second phase, which computes the full models. In the future, we will test if  
290 a first phase in which only the vertical viscosity is computed could a speed up the second phase, and hopefully reduce it to one iteration.

We did not assess the effect of the errors at the coupling interface on the simulated climate, in terms of means and variability at monthly to multi-decadal time scales. The internal feedbacks in a climate model make the impact uncertain. If the model with the legacy lagged coupling scheme computes, for instance, a too high interface temperature at a given time step, the  
295 atmosphere to ocean heat fluxes of the following time step will be reduced accordingly and compensate the error, with a time lag. A modification of the diurnal cycle can be expected. But the error might be somewhat reduced when considering diurnal means, or longer time scales. How the long term means and variability, which are the properties analyzed by climatologists, will be affected? To assess this impact, two ensembles of climate simulations, with and without Schwarz, should be compared. The model with the Schwarz iterative method is currently too expensive for us to carry out this set of experiments. We will  
300 try to reduced this cost before carrying out a comprehensive assessment, mainly by improving the first guess, and limiting the Schwarz method to a few iterations.

*Code and data availability.* All code and data relative to this study are available at <https://doi.org/10.5281/zenodo.4273949> (Marti et al., 2020). This Digital Object (DOI) Identifier points to three files. Marti-GMD-2020-307\_Models.tar.zip is a gzipped tar file of 100 MB with the model code and scripts needed to run the model (Fortran, C++ and bash). Marti-GMD-2020-307\_Figures.zip is a zip file of 7.4 MB  
305 containing the scripts needed to produce the figures: one Ferret script and four Jupiter Python Notebooks. Marti-GMD-2020-307\_Data.tar.zip is a a gzipped tar file of 6.5 GB with the model outputs needed to produce the figures.

We give in the following more references for the code used. LMDZ, XIOS, NEMO and ORCHIDEE are released under the terms of the CeCILL license. OASIS-MCT is released under the terms of the Lesser GNU General Public License (LGPL). We used model version IPSLCM6.1.9-LR, which is build from the following model components and utilities (svn branches and tags) :

- 310
- NEMO : branches/2015/nemo\_v3\_6\_STABLE/NEMOGCM, Tag : 9455
  - ORCA1 config : trunk/ORCA1\_LIM3\_PISCES, Tag : 278
  - IPSLCM6 : CONFIG/UNIFORM/v6/IPSLCM6, Tag : 4313
  - ORCHIDEE : tags/ORCHIDEE\_2\_0/ORCHIDEE, Tag : 5661
  - OASIS : branches/OASIS3-MCT\_2.0\_branch/oasis3-mct, Tag : 1818



- 315 – IOIPSL : `IOIPSL/tags/v2_2_4/src`, Tag : HEAD
- LMDZ : `LMDZ6/branches/IPSLCM6.0.15`, Tag : 3427
- libIGCM : `trunk/libIGCM`, Tag : 1478
- XIOS : `XIOS/branchs/xios-2.5`, Tag : 1550

Model documentation is available at [https://forge.ipsl.jussieu.fr/igcmg\\_doc/wiki/Doc](https://forge.ipsl.jussieu.fr/igcmg_doc/wiki/Doc). The code modifications made in IPSL-CM6.1.9-LR to  
320 build IPSL-CM6-SW-VLR and implement the Schwarz iterative method are fully documented at <https://forge.ipsl.jussieu.fr/cocoa>.

*Author contributions.* Olivier Marti co-designed the study, runs some experiments, made the analysis and wrote the paper with large inputs by Sébastien Lemérarié and Sophie Valcke. Sébastien Nguyen helped to design the study, made all the coding to implement the Schwarz method, run some experiments and made some analysis. Pascale Braconnot co-designed the study. Sophie Valcke brought her expertise in coupling. Florian Lemarié and Eric Blayo designed the mathematical framework and brought their expertise in all mathematical aspects.

325 *Competing interests.* Authors declare no competing interests.

*Acknowledgements.* This study is part of the ANR project COCOA (<https://anr.fr/Projet-ANR-16-CE01-0007>). This work was granted access to the HPC resources of TGCC under allocation made by GENCI (Grand Équipement National de Calcul Intensif, grant 2019-A0040100239). It benefits from the development of the common modelling IPSL infrastructure coordinated by the IPSL climate modeling center (<https://cmc.ipsl.fr>). Data files were prepared with NCO (netCDF Operators, Zender, 2008, and <http://nco.sourceforge.net>). Sketches  
330 are drawn with LibreOffice (<https://www.libreoffice.org>). Histograms are produced with Matplotlib (Hunter, 2007, and <https://matplotlib.org>) in Jupyter Python notebooks. Maps were drawn with pyFerret, a product of NOAA's Pacific Marine Environmental Laboratory (<http://ferret.pmel.noaa.gov/Ferret>). Patrick Brockman and Jean-Yves Peterschmitt brought invaluable help in the realisation of the figures.





## References

- Balaji, V., Anderson, J., Held, I., Winton, M., Durachta, J., Malyshev, S., and Stouffer, R. J.: The Exchange Grid, in: *Parallel Computational Fluid Dynamics 2005*, pp. 179–186, Elsevier, <https://doi.org/10.1016/B978-044452206-1/50021-5>, <https://linkinghub.elsevier.com/retrieve/pii/B9780444522061500215>, 2006.
- Boucher, O., Servonnat, J., Albright, A. L., Aumont, O., Balkanski, Y., Bastrikov, V., Bekki, S., Bonnet, R., Bony, S., Bopp, L., Braconnot, P., Brockmann, P., Cadule, P., Caubel, A., Cheruy, F., Codron, F., Cozic, A., Cugnet, D., D’Andrea, F., Davini, P., Lavergne, C., Denvil, S., Deshayes, J., Devilliers, M., Ducharne, A., Dufresne, J., Dupont, E., Éthé, C., Fairhead, L., Falletti, L., Flavoni, S., Foujols, M., Gardoll, S., Gasteineau, G., Ghattas, J., Grandpeix, J., Guenet, B., Guez, E., L., Guilyardi, E., Guimberteau, M., Hauglustaine, D., Hourdin, F., Idelkadi, A., Joussaume, S., Kageyama, M., Khodri, M., Krinner, G., Lebas, N., Levvasseur, G., Lévy, C., Li, L., Lott, F., Lurton, T., Luysaert, S., Madec, G., Madeleine, J., Maignan, F., Marchand, M., Marti, O., Mellul, L., Meurdesoif, Y., Mignot, J., Musat, I., Ottlé, C., Peylin, P., Planton, Y., Polcher, J., Rio, C., Rochetin, N., Rousset, C., Sepulchre, P., Sima, A., Swingedouw, D., Thiéblemont, R., Traore, A. K., Vancoppenolle, M., Vial, J., Vialard, J., Viovy, N., and Vuichard, N.: Presentation and Evaluation of the IPSL-CM6A-LR Climate Model, *J. Adv. Model. Earth Syst.*, 12, <https://doi.org/10.1029/2019MS002010>, <https://onlinelibrary.wiley.com/doi/abs/10.1029/2019MS002010>, 2020.
- Braconnot, P., Marti, O., and Joussaume, S.: Adjustment and feedbacks in a global coupled ocean-atmosphere model, *Climate Dynamics*, 13, 507–519, 7-8, 1997.
- Connors, J. M. and Ganis, B.: Stability of algorithms for a two domain natural convection problem and observed model uncertainty, *Comput Geosci*, 15, 509–527, <https://doi.org/10.1007/s10596-010-9219-x>, <http://link.springer.com/10.1007/s10596-010-9219-x>, 2011.
- Dufresne, J.-L., Foujols, M.-A., Denvil, S., Caubel, A., Marti, O., Aumont, O., Balkanski, Y., Bekki, S., Bellenger, H., Benschila, R., Bony, S., Bopp, L., Braconnot, P., Brockmann, P., Cadule, P., Cheruy, F., Codron, F., Cozic, A., Cugnet, D., Noblet, N., Duvel, J.-P., Ethé, C., Fairhead, L., Fichefet, T., Flavoni, S., Friedlingstein, P., Grandpeix, J.-Y., Guez, L., Guilyardi, E., Hauglustaine, D., Hourdin, F., Idelkadi, A., Ghattas, J., Joussaume, S., Kageyama, M., Krinner, G., Labetoulle, S., Lahellec, A., Lefebvre, M.-P., Lefevre, F., Levy, C., Li, Z. X., Lloyd, J., Lott, F., Madec, G., Mancip, M., Marchand, M., Masson, S., Meurdesoif, Y., Mignot, J., Musat, I., Parouty, S., Polcher, J., Rio, C., Schulz, M., Swingedouw, D., Szopa, S., Talandier, C., Terray, P., Viovy, N., and Vuichard, N.: Climate change projections using the IPSL-CM5 Earth System Model: from CMIP3 to CMIP5, *Climate Dynamics*, 40, 2123–2165, <https://doi.org/10.1007/s00382-012-1636-1>, <http://link.springer.com/10.1007/s00382-012-1636-1>, 2013.
- Eyring, V., Bony, S., Meehl, G. A., Senior, C. A., Stevens, B., Stouffer, R. J., and Taylor, K. E.: Overview of the Coupled Model Intercomparison Project Phase 6 (CMIP6) experimental design and organization, *Geoscientific Model Development*, 9, 1937–1958, <https://doi.org/10.5194/gmd-9-1937-2016>, <https://www.geosci-model-dev.net/9/1937/2016/>, 2016.
- Gander, M. J. and Halpern, L.: Optimized Schwarz waveform relaxation methods for advection reaction diffusion problems, *SIAM J. Numer. Anal.*, 45, 2007.
- Gander, M. J., Halpern, L., and Nataf, F.: Optimal Convergence for Overlapping and Non-Overlapping Schwarz Waveform Relaxation, in: *Proceedings of the 11th International Conference on Domain Decomposition Methods*, edited by Lai, C.-H., Bjørstad, P., Cross, M., and Widlund, O., 1999.
- Gross, M., Wan, H., Rasch, P. J., Caldwell, P. M., Williamson, D. L., Klocke, D., Jablonowski, C., Thatcher, D. R., Wood, N., Cullen, M., Beare, B., Willett, M., Lemarié, F., Blayo, E., Malardel, S., Termonia, P., Gassmann, A., Lauritzen, P. H., Johansen, H., Zarzycki, C. M., Sakaguchi, K., and Leung, R.: Physics–Dynamics Coupling in Weather, Climate, and Earth System Models: Challenges and



- 370 Recent Progress, *Monthly Weather Review*, 146, 3505–3544, <https://doi.org/10.1175/MWR-D-17-0345.1>, <http://journals.ametsoc.org/doi/10.1175/MWR-D-17-0345.1>, 2018.
- Hunter, J. D.: Matplotlib: A 2D graphics environment, *Computing in Science & Engineering*, 9, 90–95, <https://doi.org/10.1109/MCSE.2007.55>, publisher: IEEE Computer Soc., 2007.
- Keyes, D. E., McInnes, L. C., Woodward, C., Gropp, W., Myra, E., Pernice, M., Bell, J., Brown, J., Clo, A., Connors, J., Constantinescu, E., Estep, D., Evans, K., Farhat, C., Hakim, A., Hammond, G., Hansen, G., Hill, J., Isaac, T., Jiao, X., Jordan, K., Kaushik, D., Kaxiras, E., Koniges, A., Lee, K., Lott, A., Lu, Q., Magerlein, J., Maxwell, R., McCourt, M., Mehl, M., Pawlowski, R., Randles, A. P., Reynolds, D., Rivière, B., Rüde, U., Scheibe, T., Shadid, J., Sheehan, B., Shephard, M., Siegel, A., Smith, B., Tang, X., Wilson, C., and Wohlmuth, B.: Multiphysics simulations: Challenges and opportunities, *The International Journal of High Performance Computing Applications*, 27, 4–83, <https://doi.org/10.1177/1094342012468181>, <http://journals.sagepub.com/doi/10.1177/1094342012468181>, 2013.
- 375 Lemarié, F.: Algorithmes de Schwarz et couplage océan-atmosphère, Ph.D. thesis, Université Joseph Fourier, Grenoble, 2008.
- Lemarié, F., Debreu, L., and Blayo, E.: Toward an Optimized Global-in-Time Schwarz Algorithm for Diffusion Equations with Discontinuous and Spatially Variable Coefficients, Part 1: The Constant Coefficients Case, *Electron. Trans. Numer. Anal.*, 40, 148–169, publisher: Kent State University Library, 2013.
- Lemarié, F., Marchesiello, P., Debreu, L., and Blayo, E.: Sensitivity of ocean-atmosphere coupled models to the coupling method : example of tropical cyclone Erica, Research Report 8651, INRIA, <https://hal.inria.fr/hal-00872496v6/document>, 2014.
- 380 Lemarié, F., Blayo, E., and Debreu, L.: Analysis of Ocean-atmosphere Coupling Algorithms: Consistency and Stability, *Procedia Computer Science*, 51, 2066–2075, <https://doi.org/10.1016/j.procs.2015.05.473>, <http://linkinghub.elsevier.com/retrieve/pii/S1877050915012818>, 2015.
- Locarnini, R. A., Mishonov, A. V., Antonov, J. I., Boyer, T. P., Garcia, H. E., Baranova, O. K., Zweng, M. M., Paver, C. R., Reagan, J. R., Johnson, D. R., Hamilton, M., and Seidov, D.: World Ocean Atlas 2013, Volume 1: Temperature., S. Levitus, Ed.; A. Mishonov, Tech. Ed; NOAA Atlas NESDIS 73, NOAA, 2013.
- 390 Marti, O., Braconnot, P., Dufresne, J.-L., Bellier, J., Benschila, R., Bony, S., Brockmann, P., Cadule, P., Caubel, A., Codron, F., de Noblet, N., Denvil, S., Fairhead, L., Fichet, T., Foujols, M.-A., Friedlingstein, P., Goosse, H., Grandpeix, J.-Y., Guilyardi, E., Hourdin, F., Idelkadi, A., Kageyama, M., Krinner, G., Lévy, C., Madec, G., Mignot, J., Musat, I., Swingedouw, D., and Talandier, C.: Key features of the IPSL ocean atmosphere model and its sensitivity to atmospheric resolution, *Clim Dyn*, 34, 1–26, <https://doi.org/10.1007/s00382-009-0640-6>, <http://link.springer.com/10.1007/s00382-009-0640-6>, 2010.
- 395 Marti, O., Nguyen, S., Braconnot, P., Valcke, S., Lemarié, F., and Blayo, E.: A Schwarz iterative method to evaluate ocean- atmosphere coupling schemes. Implementation and diagnostics in IPSL-CM6-SW-VLR. GMD-2020-307, <https://doi.org/10.5281/zenodo.4273949>, <https://zenodo.org/record/4273949>, type: dataset, 2020.
- 400 Pelletier, C., Lemarié, F., and Blayo, E.: Sensitivity analysis and metamodels for the bulk parametrization of turbulent air-sea fluxes, *Q.J.R. Meteorol. Soc.*, 144, 658–669, <https://doi.org/10.1002/qj.3233>, <http://doi.wiley.com/10.1002/qj.3233>, 2018.
- Rousset, C., Vancoppenolle, M., Madec, G., Fichet, T., Flavoni, S., Barthélemy, A., Benschila, R., Chanut, J., Levy, C., Masson, S., and Vivier, F.: The Louvain-La-Neuve sea ice model LIM3.6: global and regional capabilities, *Geoscientific Model Development*, 8, 2991–3005, <https://doi.org/10.5194/gmd-8-2991-2015>, <http://www.geosci-model-dev.net/8/2991/2015/>, 2015.
- 405 Sepulchre, P., Caubel, A., Ladant, J.-B., Bopp, L., Boucher, O., Braconnot, P., Brockmann, P., Cozic, A., Donnadieu, Y., Dufresne, J.-L., Estella-Perez, V., Ethé, C., Fluteau, F., Foujols, M.-A., Gastineau, G., Ghattas, J., Hauglustaine, D., Hourdin, F., Kageyama, M., Khodri, M., Marti, O., Meurdesoif, Y., Mignot, J., Sarr, A.-C., Servonnat, J., Swingedouw, D., Szopa, S., and Tardif, D.: IPSL-CM5A2 – an Earth



- system model designed for multi-millennial climate simulations, *Geosci. Model Dev.*, 13, 3011–3053, <https://doi.org/10.5194/gmd-13-3011-2020>, <https://gmd.copernicus.org/articles/13/3011/2020/>, 2020.
- 410 Théry, S., Pelletier, C., Lemarié, F., and Blayo, E.: Analysis of Schwarz Waveform Relaxation for the Coupled Ekman Boundary Layer Problem with Continuously Variable Coefficients, <https://hal.inria.fr/hal-02544113>, 2020.
- Zender, C. S.: Analysis of self-describing gridded geoscience data with netCDF Operators (NCO), *Environmental Modelling & Software*, 23, 1338–1342, <https://doi.org/10.1016/j.envsoft.2008.03.004>, <https://linkinghub.elsevier.com/retrieve/pii/S1364815208000431>, 2008.